Optimal Battery Energy Storage System Management with Wind Turbine Generator in Unbalanced Low Power Distribution System

Samarjit PATNAIK [1] , *Manas Ranjan NAYAK* [1] , *Meera VISWAVANDYA* [2]

[1]Department of Electrical Engineering, Biju Patnaik University of Technology,
Chhend, 769015 Rourkela, Odisha, India
[2]Department of Electrical Engineering, Odisha University of Technology and Research,
Kalinga Vihar, 751003 Bhubaneswar, Odisha, India

patnaik.samarjit@gmail.com, manasnk72@gmail.com, mviswavandya@cet.edu.in

Abstract. *Wind Turbine Generators (WTG) are being integrated into distribution systems on a large scale worldwide as part of a global effort to capture green energy. Wind turbine generator intermittency may be mitigated by Battery Energy Storage Systems (BESS), which have emerged as a viable option in recent years. To find the best position and capacity for wind power generation and BESS charging/discharging dispatches, a Red Fox Optimisation (RFO) algorithm is used while optimising the imbalanced distribution network's performance under technological restrictions. The charging or discharging criteria for this method is the average feeder load. The charging techniques for BESS using WTG and Sustainable Average Load (SAL) are evaluated in terms of the free-running mode of dispatch cycle. The suggested approach is tested on an IEEE-37 bus Unbalanced Radial Distribution Network (UDN). It has been shown that the suggested method enhances several performance objectives of the distribution system.*

Keywords

Wind Turbine Generator, IEEE-37 bus unbalanced radial distribution network, Red Fox Optimisation algorithm, Sustainable Average Load.

1. Introduction

Wind energy generation as a form of Renewable Energy Source (RES) has been driven by concerns over climate change and global warming. The renewable energy sources provide several other technical, economic, and environmental advantages, such as reduction of system power losses and the enhancement of system's reliability [1]. The regulators have put regulatory requirements on the distribution system to promote the integration of renewable energy sources or Distributed Generators (DG) [2]. The responsibility of distribution companies [3] is to deliver sustainable, affordable, and safe energy by anticipating consumer requirements and it becomes even more challenging with increasing DG penetration [4].

The Wind Turbine Generator (WTG) as a DG can take part in grid connected mode to provide green power to consumers, while ensuring that they remain operational at all times. The major challenge of integrating WTG is the intermittent nature of wind energy. In-spite of several difficulties, the WTG penetration into India's distribution system has risen over the years. The difficulty of WTG integration further escalates in an unbalanced distribution systems because of the uncertain nature of both generation and loads, as well as the degree to which the distribution systems are unbalanced [5].

The inclusion of storage elements like Battery Energy Management System (BESS), with proper power management strategy can resolve the intermit-

tency or uncertainty up-to a large extend [6] and [7]. In addition, proper BESS management provides economic benefits to consumers by peak shifting strategy. While designing energy storage systems, demand load studies, reliability, and continuity have all been considered [8] and [9].

The power loss reduction and improvement in voltage profiles can be achieved by integrating WTG and BESS into the Unbalanced Radial Distribution Network (UDN) [10]. Several equality and inequality constraints must be considered when allocating WTG and BESS optimally [11], [12], [13], [14], and [15]. Various 3-phase power flow algorithms are utilised in the literature and are based on the backward-forward flow algorithm, which encompasses total load and three-phase branch modelling. The authors of [16] established a three-phase unbalanced load flow technique based on P-V and P-Q models, while [17] proposed a unified three-phase power-flow model for unbalanced distribution system analysis with DGs.

The paper [18] presented a two-stage strategy for lowering the effect of RESs uncertainty on imbalanced systems, but it only evaluated the best and worst generation situations and did not account for load uncertainties. In [19], the optimum location and size of DGs in unbalanced RDS system were determined with just load uncertainties taken into account. In [20], the optimum allocation of RESs, both Photovoltaic (PV) and Wind Turbine (WT), was performed considering load and generation uncertainties using randomly selected samples for simulating generation uncertainty; these studies were only applied to balanced distribution systems.

In [21] and [22], only WTGs with a specific capacity were optimally placed in unbalanced distribution systems based on generation and load uncertainties. In this study, however, the author neglected shunt admittance of transmission line and system voltage regulators, as well as considering unity DG power factor, to simplify the planning problem.

None of the reviewed literature or recent work have focused on BESS management strategy evaluation and DG placement in unbalanced system simultaneously. Considering the scope of research, the major objectives of optimising voltage deviation and minimising power losses, the suggested BESS management technique generates the ideal location/size/type specifications for WTG and BESS. Further, the comparison between free-running discharge and sustainable average load discharge is formulated. As a result, a very intelligent and robust computational tool is necessary for an effective and dependable solution.

A Red Fox Optimisation (RFO) technique is used in this study to optimise the system's performance objectives. The following are the primary contributions of this manuscript:

- This study examines the unbalanced power flow operation during dynamic load intervals in distribution systems for controlling storage and wind production.

- A novel RFO method is used to effectively solve highly nonlinear power system problems.

- A novel weighted sum technique is provided for combining several objective targets.

- This study provides information on methodology used to maximise the efficiency of energy storage systems.

- This study examines the IEEE-37 bus and IEEE-25 bus UDN performance criteria for two operational ways of BESS.

The rest of the paper is organised in the following manner. Sections 2. and Sec. 3. have been devoted to system modelling and energy management strategies, respectively. Section 4. explains the framing of objective function solving the problem. Section 5. describes the RFO algorithm and its implementation. Section 6. discusses the simulation findings and their interpretation. Finally, the conclusion is presented in Sec. 7.

2. System Modelling

WTG shares the power to the grid by cascading an AC/DC converter and a DC/AC converter. The BESS generates electricity using a bidirectional DC/DC battery converter and connects to the grid via a bidirectional inverter. A shared bus connects the WTG and BESS to the grid. The $P_{Grid,i}^{K(t)}$, and $Q_{Grid,i}^{K(t)}$ indicates the active and reactive power interaction with the grid from WTG and BESS microgrid subsystem, at time instant t for the Kth phase. The battery converter works as a charge controller throughout the BESS's charging procedure. The system configuration is shown in Fig. 1.

2.1. Load Modelling

The load demand for the system under study is modelled using average normalised hourly load weight factors for one day. The weight variables for each hour of the day are shown in Fig. 2.

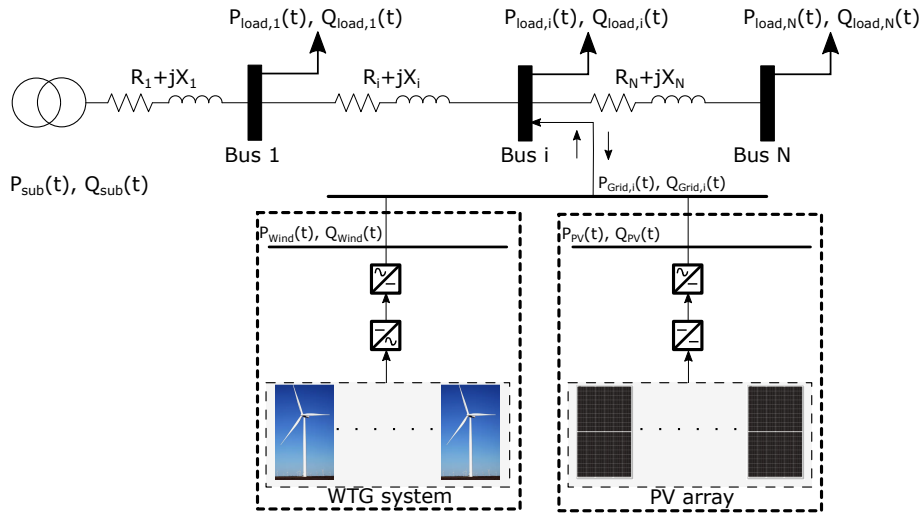The predicted load on a bus at any given moment may be calculated as per Eq. (1) and Eq. (2):

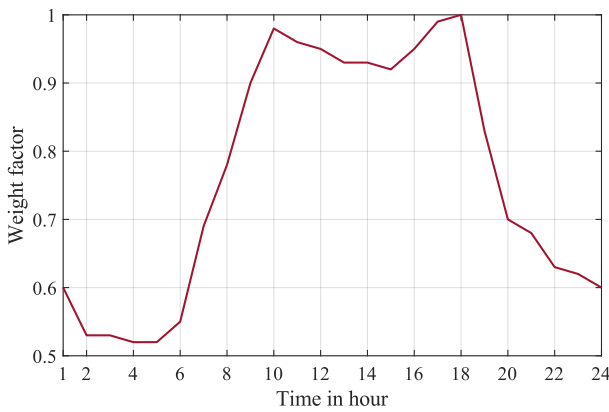**Fig. 1:** Radial distribution system with WTG and BESS.

Fig. 2: Hourly weight factor for a day.

$$P_{Load,p}^k(t) = w_h(t) \cdot P_p^k, \qquad (1)$$

$$Q_{Load,p}^k(t) = w_h(t) \cdot Q_p^k, \qquad (2)$$

where $w_h(t)$ is the hourly weight factor. P_p^k and Q_p^k are maximum active and reactive load at bus p, respectively. k is the number of phases of the system.

2.2. WTG Modelling

With a constant power factor input, WTG is handled as a negative PQ load throughout the power flow algorithm. The wind turbine is integrated into the power flow process by deducting the required PQ values for actual and reactive wind energy output from UDN's bus load. In this study, the WTG real power, reactive power and power factor are 100 kW, ±45 kVAR and 0.9, respectively. For example, in Fig. 3, the wind energy generation is both active and reactive.

2.3. BESS Modelling

The BESS charging and discharging is modelled as a three-phase real power at any time. During battery charging, actual energy generated by WTG is added directly to the battery's energy level and is not viewed as a negative load. When the battery is discharged, it is removed from the bus, and the WTG and battery are considered unfavourable.

The State of Charge (SOC) is expressed as a function of BESS energy capacity as per the below Eq. (3),

$$SOC = 1 - \frac{E_{bat}}{E_{bat,cap}}, \; 0 \le SOC \le 1, \qquad (3)$$

where E_{bat} is the battery energy for any given time instant. The change in the state of charge is a function of the self-discharge factor, and it is expressed as per Eq. (4):

$$SOC(t + dt) = $$
$$= SOC(t) + \frac{E_{bat}}{E_{bat,cap}} - D(SOC(t)). \qquad (4)$$

2.4. Distribution Network Modelling

The load flow analysis for the unbalanced distribution network under study is carried out using the backward-forward sweep algorithm. The backward-forward sweep algorithm is applied to the 3-phase unbalanced network considering the line mutual impedance and load parameters. The mathematical formulation is discussed in [23] and [24] served as the basis for UDN load flow analysis. The current at a node may be computed as per Eq. (5).
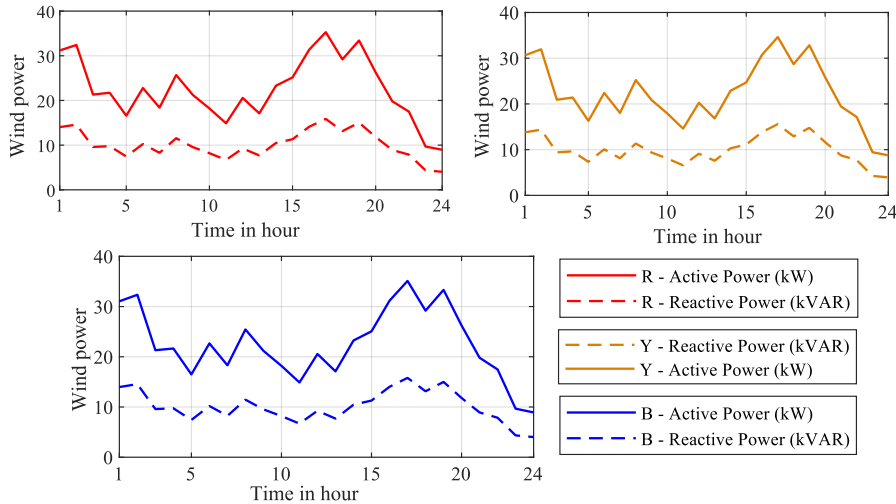
Fig. 3: Active and reactive power generation from WTG in a day.

$$[I_{ij}^{RYB}] = [I_j^{RYB}] =$$
$$= [I_{j_{load}}^{RYB}] + [I_{j_{DG}}^{RYB}] + \sum_{jk \epsilon E(G)} [I_{jk}^{RYB}], \quad (5)$$

where, $[I_{ij}^{RYB}]$ is the phase current matrix across line ij, $[I_{j_{DG}}^{RYB}]$ is the DG injected current in three phases at node j, $[I_j^{RYB}]$ is the Load demand injected current in three phases at node j, G is the Distribution system topology, $V(G)$ is the Node collection and $E(G)$ is the Branch collection.

Three kinds of loads exist constant power, constant current, and constant impedance. Each iteration will update the power of the load and the voltage till the divergence between the substation voltage received through backward sweep and the preset voltage is within the tolerance. In planning, these approaches calculate the three-phase voltages at every node and the 3-phase currents at each branch.

3. Energy Management Strategy

While in one mode, the WTG are shut down to store energy, in the other, the feeder and the batteries are both used to charge batteries when demand falls below a specific level. As soon as the load surpasses this threshold, energy from the WTG is used to meet the load's demand, and the battery is depleted to reduce the amount of load that must be handled by the source node at the substation's bulk power. Because the system is trying to keep the observed substation load as near to the preset figure as feasible, this is the consequence. Free running has also been explored as a technique of depleting a battery's battery life.
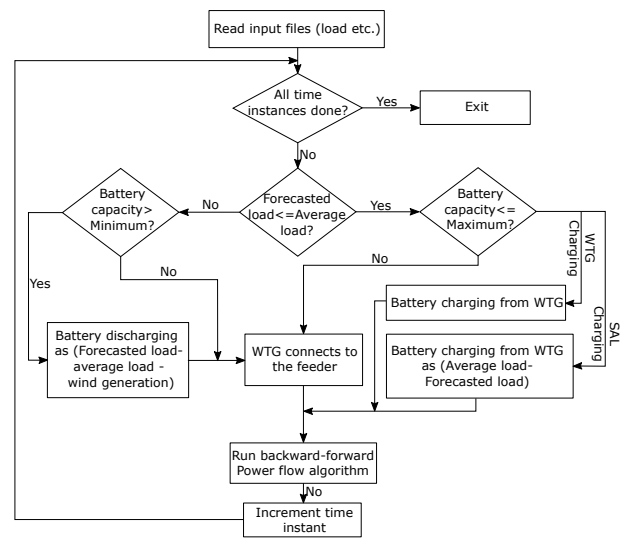

Fig. 4: Flow chart for BESS dispatch operation for free running discharging only.

For free-running discharge, Fig. 4 depicts the battery dispatch flow chart in two modes of operation. First, the battery may only be charged to the stated maximum level in either charging phase, and if the load exceeds the average value, WTG is directly linked to the feeder after the battery reaches that maximum level.

4. Problem Formulation

The problem involves figuring out the best place to put WT and BESS and when they should be charged or discharged, while UDN's performance must be improved while satisfying the operating constraints.

4.1. Objective Function

The idea is to minimise distribution network power loss while also minimising voltage drift. As a result, the mathematical formulation can be expressed as combining two primary objectives. The primary objective is the reduction of power loss of distribution network, which can be expressed as:

$$F_{obj}^1 = \frac{(P_{Loss}^{RYB})^{WT+Base}}{(P_{Loss}^{RYB})^{Base}}, \tag{6}$$

$$P_{Loss}^{RYB} = P_{Loss}^R + P_{Loss}^Y + P_{Loss}^B, \tag{7}$$

$$P_{Loss}^K = \frac{\left(\sum_{pq=1}^{nbr} \sum_{t=1}^{nt} R_{pq}^K I_{pq}^{K^2}(t)\right)}{nt}, \tag{8}$$

where $I_{pq}^K(t)$ implies current, R_{pq}^K, P_{Loss}^K are the resistance and average active power loss of pq^{th} branch at instant t in K^{th} phase, nbr and nt signifies the total number of branches and time slot. P_{Loss}^{RYB} is the active power loss of the unbalanced distribution network.

The secondary objective for decreasing Voltage Deviation (VD) of the unbalanced distribution network is calculated as:

$$F_{obj}^2 = \frac{(V_{d,avg}^{RYB})^{WT+Base}}{(V_{d,avg}^{RYB})^{Base}}, \tag{9}$$

$$V_{d,avg}^{RYB} = \frac{V_d^R + V_d^Y + V_d^B}{3}, \tag{10}$$

$$V_d^k = \sum_{p=1}^{nb} \left| \frac{\sum_{t=1}^{nt} V_p^k(t)}{nt} \right|, \tag{11}$$

where V_P^K denotes voltage of pth bus in time instant t at K^{th} phase. V_d^K is the voltage deviation of the Kth phase. nb denotes the total bus number. $V_{d,avg}^{RYB}$ imply average VD of the 3-phase system.

The overall objective function of the system can be expressed as: Minimize(F_{obj}), where:

$$F_{obj} = a \cdot F_{obj}^1 + b \cdot F_{obj}^2, \tag{12}$$

$$a = \frac{F_{obj}^2}{F_{obj}^1 + F_{obj}^2}, \ b = \frac{F_{obj}^1}{F_{obj}^1 + F_{obj}^2}. \tag{13}$$

4.2. System Constraints

The system works within the confines of the following limits on equality and inequity:

$$P_{sub}^K(t) = P_{Load}^K(t) + P_{Loss}^K(t) + P_{Wind}^K(t) \mp P_{bat}^K(t), \tag{14}$$

$$Q_{sub}^K(t) = Q_{Load}^K(t) + Q_{Loss}^K(t) + Q_{Wind}^K(t) \mp Q_{bat}^K(t), \tag{15}$$

$$V_p^{K,\min} \leq V_p^K(t) \leq V_p^{K,\max}, \tag{16}$$

$$I_{pq}^K(t) \leq I_{pq}^{K,\max}, \tag{17}$$

$$SOC^{\min} \leq SOC(t) \leq SOC^{\max}, \tag{18}$$

where $P_{sub}^K(t)$, $P_{Load}^K(t)$, $P_{Loss}^K(t)$, $P_{Wind}^K(t)$, & $P_{bat}^K(t)$ refers active power injection of the substation, the active load of bus, active power losses, active power of WTG, and active power of BESS respectively and similarly $Q_{sub}^K(t)$, $Q_{Load}^K(t)$, $Q_{Loss}^K(t)$, $Q_{Wind}^K(t)$, & $Q_{bat}^K(t)$ refers reactive power injection of the substation, the reactive load of bus, reactive power losses, reactive power of WTG, and reactive power of BESS, respectively, in time t in K^{th} phase. $V_p^{K,\max}$ & $V_p^{K,\min}$ signify maximum and minimum limits of the voltage of pth bus. $I_{pq}^{K,\max}$ is the maximum current of pq^{th} branch in the Kth phase.

4.3. Annual Cost of Energy Loss

The Energy Losses (ACEL) annually can be modelled as monetary value as Eq. (19).

$$ACEL = P_{Loss}^{RYB} E_c T \tag{19}$$

where, E_c denotes the energy price as 4.30 Rs·kWh^{-1}, & T denotes the duration as 8760 hours for the system under study.

5. RFO Algorithm

The algorithm is inspired by the behaviour of the red foxes. Red foxes exist in two sub-populations: those that leave the well-defined territory and those that live nomadic lives [25]. Each herd is responsible for shearing a specific region within the alpha pair hierarchy. Young foxes may leave the herd to form their group if they believe they have a good chance of taking over another area. However, if they do not leave the family, they are likely to inherit their parents' hunting territory. Red foxes are known for their skill in catching and devouring small prey. The fox hunts for food while investigating the area, concealing until he gets close enough to attack effectively. If prey is found in the far distance, the algorithm replicates the fox's exploration of territory as a global search. Assaults were conducted in the second phase by travelling over the surroundings to get as close to the prey as feasible.

5.1. Fundamental Premise

The successive iterations maintain a consistent number of foxes in the population of people. Each of

the foxes is denoted by a point $\overline{x} = (x_0, x_1, \ldots, x_{n-1})$ with n coordinates. To denote each of them as $\overline{x}^i$ in iteration t, we use notation $(\overline{x}_j^i)^t$, where t denotes the population's size, and j denotes the solution space's dimensions. We suppose that foxes traverse solution space using supplied equations to determine the criteria function's optimal values.

5.2. Search of Food

Each fox in a herd must perform a critical duty to guarantee the family's survival. Individuals go too far if there is no food available in the nearby habitat or if the herd seeks to explore new territory. They communicate the knowledge they gather throughout this expedition with family members to aid in their survival and growth. The surrounding area is explored using a model that considers each participant's fitness. We presume in the suggested manner that the best fox has investigated the most intriguing places and can share this knowledge with a community. As a result, we first sort the population by fitness condition and then computed as:

$$d\left(\left(\overline{x}^i\right)^t, \left(\overline{x}^{best}\right)^t\right) = \sqrt{\left\|\left(\overline{x}^i\right)^t - \left(\overline{x}^{best}\right)^t\right\|}, \quad (20)$$

and the foxes within a group toward the optimal one:

$$(\overline{x}^i)^t = (\overline{x}^i)^t + \alpha \ sign((\overline{x}^{best})^t - (\overline{x}^i)^t). \quad (21)$$

5.3. Traversing for Local Search

The red fox hunts for prey by patrolling its territory. Once they discover a potential victim, the fox begins to approach them in an attempt to remain undetected. In order to fool the prey into thinking it is not interested in hunting, it circles and deceives around it. It makes hasty advances to catch its prey off guard when fox is within striking distance.

As a local search phase, we used observation and mobility to deceive victims while hunting in RFO. The probability of seeing a fox as it approaches its meal was simulated by setting a random value of $\mu \in (0, 1)$ for all members in the population once every iteration, which describes the fox's behaviour as if the value is more than 0.75, move closer, and if it is less than 0.75, do not come out.

A modified Cochleoid equation represents each individual's movement when the μ parameter indicates that the population should be moved during this iteration. Two parameters define the fox observation radius

for this movement: $a \in (0, 0.2)$ is a scaling parameter that is updated once each cycle for all foxes in a population, and $\phi_0 \in (0, 2\pi)$ is a parameter that is determined at the algorithm's start for all individuals to model the fox observation angle. We use them to measure the hunting fox's field of view as:

$$r = \begin{cases} \dfrac{a \ \sin(\phi_0)}{\phi_0} & \text{if } \phi_0 \neq 0, \\ \theta & \text{if } \phi_0 = 0, \end{cases} \quad (22)$$

where θ is a random number between 0 and 1 specified first at the start of the loop, which is regarded as the impact of dire weather circumstances like fog, rain, etc. We use the following mathematical formulation for spatial coordinates to represent the movement of a whole population.

$$x_0^{new} = \arccos(\phi_1) + x_0^{actual},$$
$$x_1^{new} = \arcsin(\phi_1) + \arccos(\phi_2) + x_1^{actual},$$
$$x_2^{new} = \arcsin(\phi_1) + \arcsin(\phi_2) + \arccos(\phi_3) + x_2^{actual},$$
$$\cdots$$
$$x_{n-2}^{new} =$$
$$= \text{ar} \sum_{k=1}^{n-2} \sin(\phi_k) + \arccos(\phi_{n-1}) + x_{n-2}^{actual},$$
$$x_{n-1}^{new} =$$
$$= \arcsin(\phi_1) + \arcsin(\phi_2) + \cdots + \arcsin(\phi_{n-1}) + x_{n-1}^{actual}.$$
$$(23)$$

5.4. Herd Reproduction and Emancipation

The red fox faces several dangers in the wild. First, if food is scarce in the nearby habitat area, the animal may be relocated. Also, humans may go after the fox if it causes severe damage to a domestic animal population. There are exceptions to this rule, of course. First, because they are primarily clever, the fox herds have introduced new genetic lines due to their escape and reproduction.

Our subjective assumption is that 5 % of the population's poorest individuals are selected for each iteration to represent this behaviour to simulate tiny changes in the herd's composition. Due to their poor condition, we presume they were either relocated elsewhere or killed by hunters. In order to maintain the population's size at a consistent level, the alpha pair establishes a model of habitat territory. Two best individuals $(\overline{x}^1)^t$ and $(\overline{x}^2)^t$ represent the alpha pair in each iteration of the RFO algorithm, which calculates the habitat centre for them as per the below equation:

$$(habitat^{center})^t = \frac{(\overline{x}^1)^t + (\overline{x}^2)^t}{2}. \quad (24)$$

The squared distance between the alpha pair euclidean distance is represented as:

$$(habitat^{diameter})^t = \sqrt{\|(\overline{x}^1)^t - (\overline{x}^2)^t\|}. \qquad (25)$$

For each iteration, we randomly choose a parameter $k \in <0, 1>$, which decides whether a new nomadic individual ($k \geq 0.45$) or reproduction of the alpha pair ($k < 0.45$) will be included in the iteration. Firstly, we suppose that young individuals migrate beyond the environment as nomadic foxes to hunt and have the opportunity to breed within their herd. We randomly choose sites inside the search area but outside the habitation. We suppose that the alpha pair produces new individuals in the second scenario.

A new individual solution $(\overline{x}^{reproduced})^t$ t is created by combining two of the best solutions $(\overline{x}^1)^t$ and $(\overline{x}^2)^t$ as per Eq. (26):

$$(\overline{x}^{reproduced})^t = k\frac{(\overline{x}^1)^t + (\overline{x}^2)^t}{2}. \qquad (26)$$

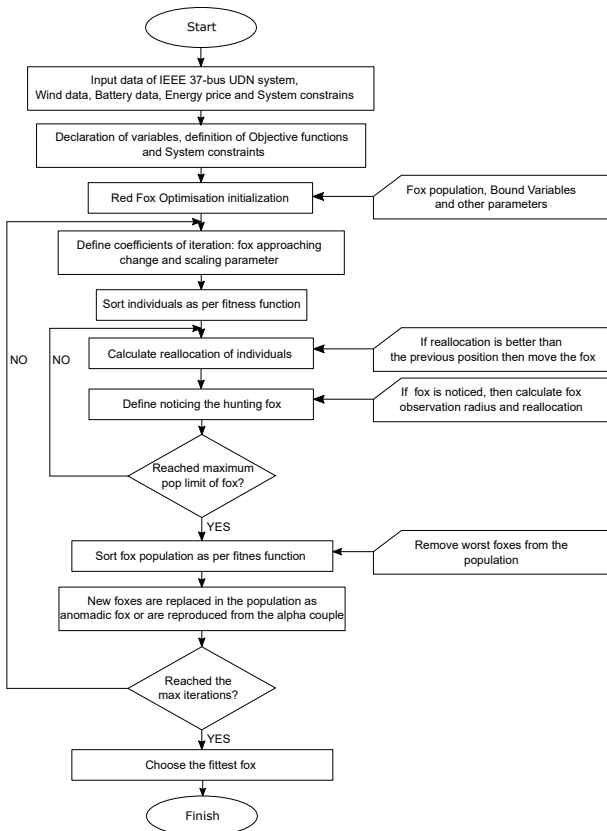We constructed our optimisation method in the manner described in Fig. (5).

Fig. 5: Flowchart of Red Fox Optimizer (RFO).

6. Simulation Results and Discussion

The suggested method is implemented on an unbalanced distribution system. In [23], the authors provides comprehensive information on the system's buses and lines for a 4.8 kV IEEE 37-bus system. The system's peak demand is around 2500 kVA and system lines are having imbalanced loads. The energy management system is also validated against IEEE 25-bus as an additional test case. The system is entirely comprised of Delta configuration lines and transformers. Using the RFO method, the maximum population count is initialised to 30, the number of iterations is initialised to 20, and the system's objective function fluctuation is presented in Fig. 6 and Fig. 7 for IEEE-37 bus and IEEE-25 bus unbalanced system, respectively. For UDN, the backward-forward algorithm is used for solving power flow.

After wind energy production, the power flow is determined using the RFO method with battery discharge values entered into the input data for establishing the best quantity and location of WTG and BESS. Since one form of charging requires battery storage to receive power from the WTG, this bus will also serve as the location of battery installation. Apart from the ease of having the full WTG on a single bus for a centralised location, the WTG may be deployed on several buses. The dispatch cycle is assumed in this research to be 24 hours long. The bus voltage limitations have been set to 5 %. $S_{base} = 25$ MVA and $V_{base} = 4.8$ kV are used as the base values in IEEE-37 bus system and IEEE-25 bus system for calculating power flow.

Three distinct instances are compared in simulation results.

- Case-1: Without Wind Turbine Generator and BESS (Base case).

- Case-2: With Wind Turbine Generator and BESS (WTG charging & Free running discharging) [Wind Turbine Generator +BESS (WTG Charging)].

- Case-3: With Wind Turbine Generator and BESS (SAL charging & Free running discharging) [Wind Turbine Generator +BESS (SAL charging)].

Table 1 and Tab. 2 summarize the application findings for the suggested strategy for optimum size and positioning of WTG and BESS in IEEE-37 bus and IEEE-25 bus unbalanced system, respectively. The Tab. 1 shows that WTG penetration is approximately 30 % of peak demand. The number of BESS units is 40 and 92 in IEEE-37 bus and IEEE-25 bus system, respectively.

**Tab. 1:** Results of the optimal solution for sizing & placement of WTG with BESS (IEEE-37 bus).

Case	Objective function value (F_{obj}) in p.u.	WTG with BESS location bus	Number of WTG units	Number of BESS units
Case-1: Base case (Without Wind Turbine Generator and BESS)	-	-	-	-
Case-2: Wind Turbine Generation with BESS (WTG charging)	0.768713	32	8	40
Case-3: Wind Turbine Generation with BESS (SAL charging)	0.740603	32	8	40

Tab. 2: Results of the optimal solution for sizing & placement of WTG with BESS (IEEE-25 bus).

Case	Objective function value (F_{obj}) in p.u.	WTG with BESS location bus	Number of WTG units	Number of BESS units
Case-1: Base case (Without Wind Turbine Generator and BESS)	-	-	-	-
Case-2: Wind Turbine Generation with BESS (WTG charging)	0.80002	23	20	92
Case-3: Wind Turbine Generation with BESS (SAL charging)	0.78537	23	20	92
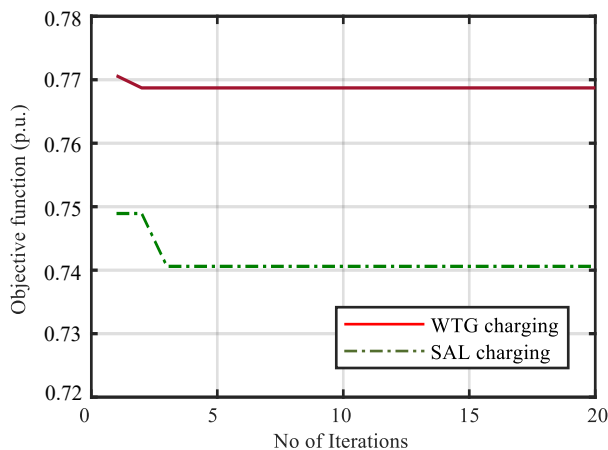
Fig. 6: Results of the objective function for WTG charging & SAL charging (IEEE-37 bus).
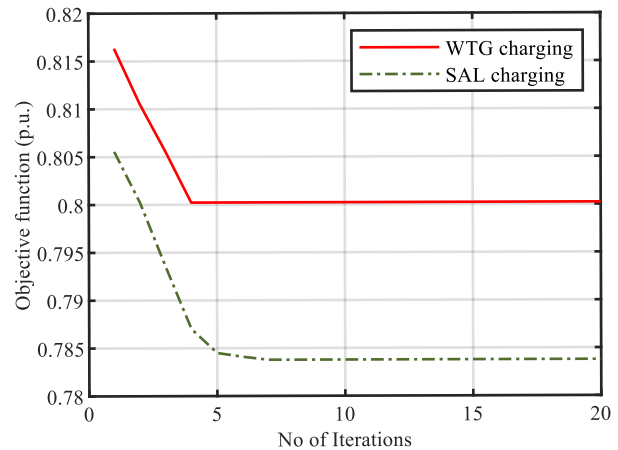
Fig. 7: Results of the objective function for WTG charging & SAL charging (IEEE-25 bus).

The voltage profiles of the IEEE-37 bus UDN system during peak hours are given in Fig. 8, Fig. 9, Fig. 10, and Fig. 11 for the Phase -R, Phase -Y, Phase -B, and 3-phase systems, respectively. The voltage profiles of the IEEE-25 bus UDN system during peak hours are given in Fig. 12, Fig. 13, Fig. 14, and Fig. 15 for the Phase -R, Phase -Y, Phase -B, and 3-phase systems, respectively. The voltage across nodes improve significantly for the system under consideration, and all the node voltages stay below predetermined range of 5 %. The gain in node voltage attained with SAL charging compared to BESS charging with WTG and the base scenario.

Figure 16 and Fig. 17 illustrate the fluctuation in a three-phase system's active and reactive power loss over a day in a IEEE-37 bus UDN system. The active and reactive losses in Case-2 are equal to those in Case-1 during the first seven hours, when the BESS charging operation occurs. Figures 18 and Fig. 19 illustrate the fluctuation in a three-phase system's active and reactive power loss over a day in a IEEE-25 bus UDN system.

Figure 20 and Fig. 21 illustrate the state of charge after one cycle, which changes between the predefined lower and higher limits throughout a complete dispatch

Tab. 3: Performance analysis of the system (IEEE-37 bus).

Parameter	Phase	Case-1	Case-2	Case-3
Lowest voltage, Bus Location	R	0.9847, 32	0.9886, 32	0.9891, 32
	Y	0.9906, 14	0.9912, 14	0.9913, 14
	B	0.9849, 34	0.9892, 30	0.9891, 30
	3-phase (RYB)	0.9894, 34	0.9928, 29	0.9931, 29
Active power loss (kW)	R	9.052	5.562	5.403
	Y	8.043	5.772	5.698
	B	11.293	7.340	7.324
	3-phase (RYB)	28.388	18.674	18.425
Reactive power loss (kVAR)	R	2.998	1.762	1.678
	Y	1.714	1.349	1.320
	B	5.139	3.413	3.446
	3-phase (RYB)	9.851	6.524	6.444
Annual Cost of Energy Loss (ACEL) (INR)	R	340,974	209,539	203,539
	Y	302,971	217,427	214,636
	B	425,384	276.509	275,899
	3-phase (RYB)	1,069,319	703,449	694,070

Tab. 4: Performance analysis of the system (IEEE-25 bus).

| Parameter	Phase	Case-1	Case-2	Case-3
Lowest voltage, Bus Location	R	0.9857, 12	0.9868, 12	0.9873, 12
	Y	0.985, 12	0.9862, 12	0.9866, 12
	B	0.9837, 12	0.9849, 12	0.9856, 12
	3-phase (RYB)	0.9848, 12	0.986, 12	0.9865, 12
Active power loss (kW)	R	4.96	4.0585	3.9346
	Y	5.2466	4.2929	4.1618
	B	5.2424	4.2894	4.1585
	3-phase (RYB)	15.45	12.6408	12.255
Reactive power loss (kVAR)	R	13.4455	10.294	9.615
	Y	11.1768	8.557	7.993
	B	12.626	9.666	9.029
	3-phase (RYB)	37.248	28.517	26.637
Annual Cost of Energy Loss (ACEL) (INR)	R	186,838	152,875	148,209
	Y	197,628	161,703	156,768
	B	197,470	161,574	156,643
	3-phase (RYB)	581,936	476,153	461,621
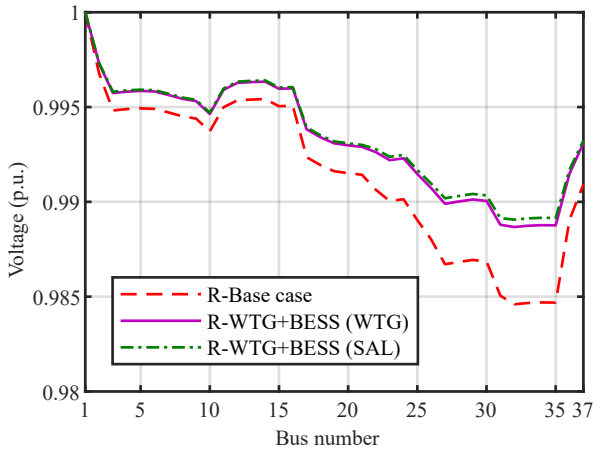
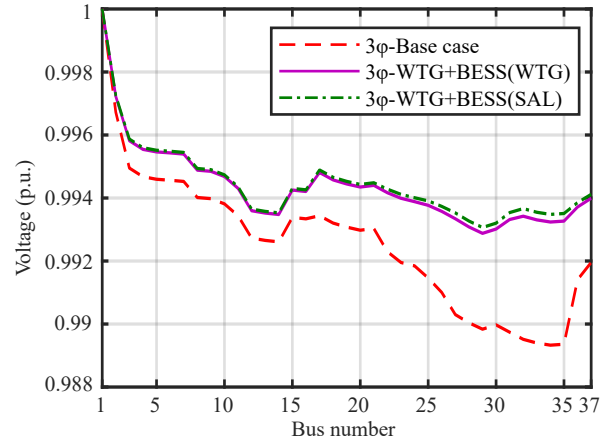**Fig. 8:** Voltage of Phase -R of the UDN system (IEEE-37 bus).

Fig. 11: 3-phase voltages of the UDN system (IEEE-37 bus).
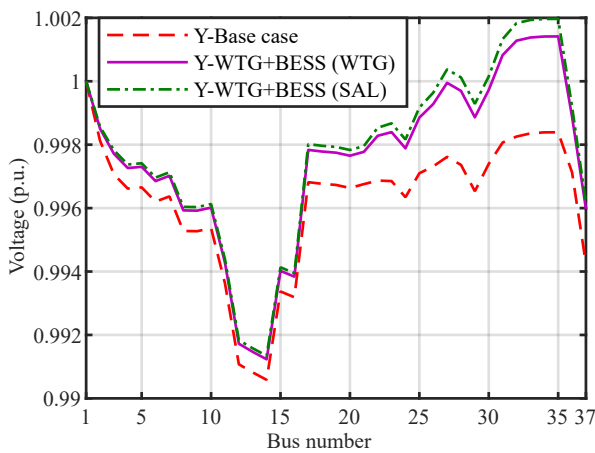

Fig. 9: Voltage of Phase -Y of the UDN system (IEEE-37 bus).
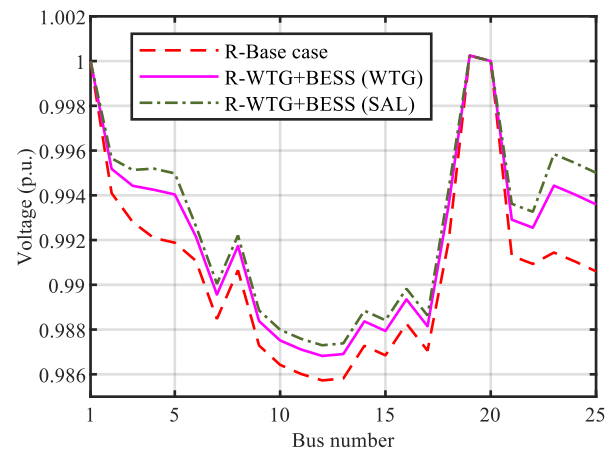

Fig. 12: Voltage of Phase -R of the UDN system (IEEE-25 bus).
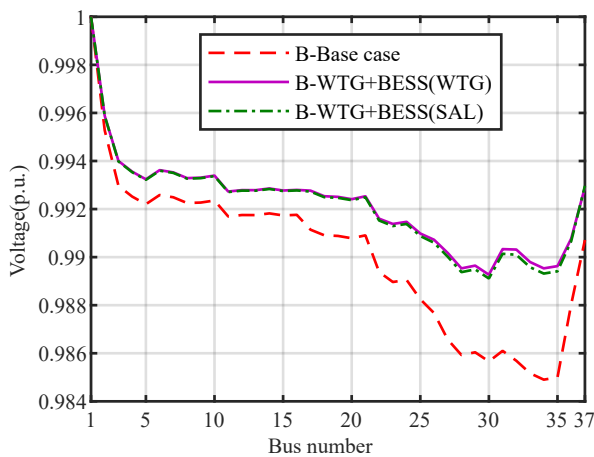

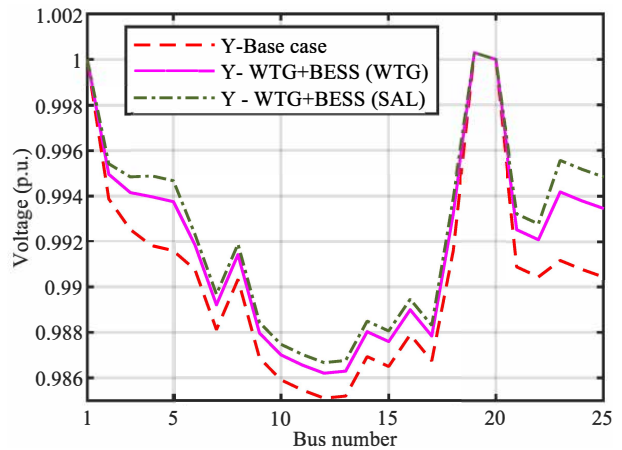**Fig. 10:** Voltage of Phase -B of the UDN system (IEEE-37 bus).

Fig. 13: Voltage of Phase -Y of the UDN system (IEEE-25 bus).

cycle in a IEEE-37 bus UDN and IEEE-25 bus UDN, respectively.

The findings of the lowest voltage with bus number, active and reactive power loss, and annual energy savings are presented in Tab. 3 and Tab. 4 for IEEE-37 bus system and IEEE-25 bus system, respectively. Both charging techniques efficiently decrease active and reactive power loss. The SAL charging technique achieves the maximum decrease in both losses. The proposed method ensures that the grid always has a positive net demand. As a consequence, no reverse power flow occurs.
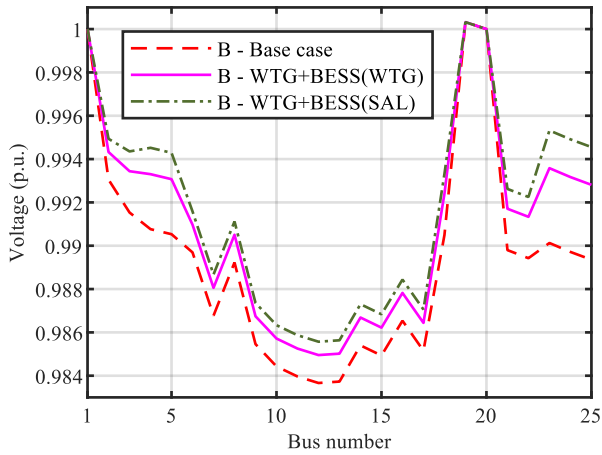
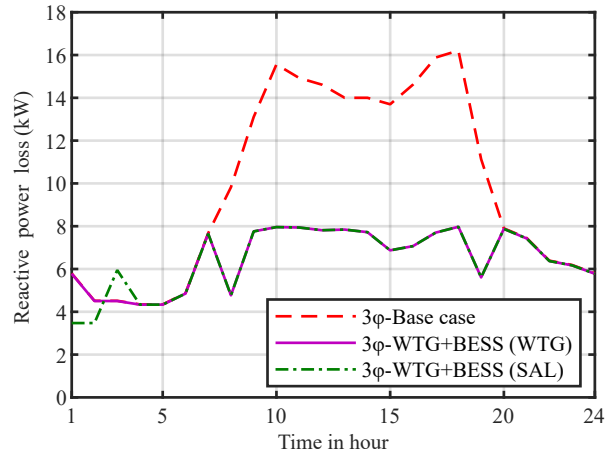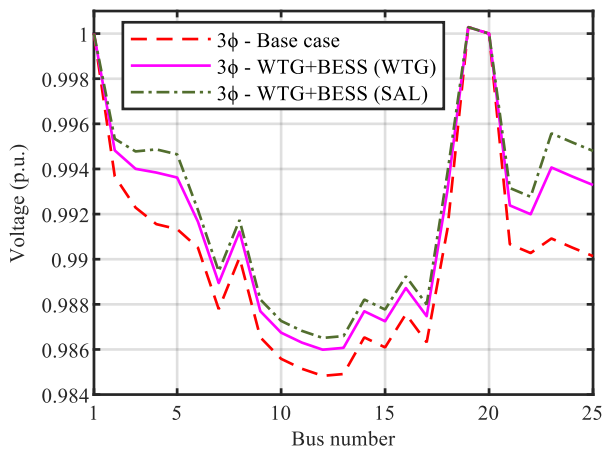**Fig. 14:** Voltage of Phase -B of the UDN system (IEEE-25 bus).

Fig. 15: 3-phase voltages of the UDN system (IEEE-25 bus).
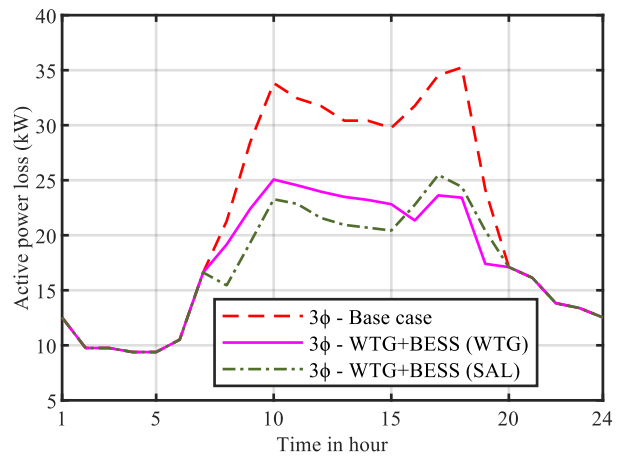

Fig. 16: 3-phase power losses (active) of the UDN system (IEEE-37 bus).

Fig. 17: 3-phase power losses (reactive) of the UDN system (IEEE-37 bus).

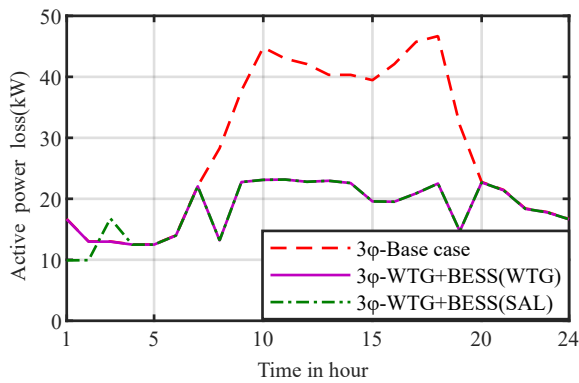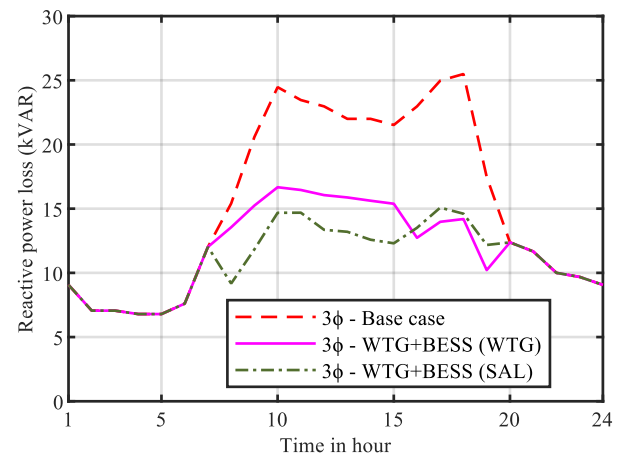**Fig. 18:** 3-phase power losses (active) of the UDN system (IEEE-25 bus).

Fig. 19: 3-phase power losses (reactive) of the UDN system (IEEE-25 bus).

Figure 22 and Fig. 23 illustrate the best charging/discharging condition of the BESS system in a IEEE-37 bus system and IEEE-25 bus system, respectively. Every 24 hours, BESS is charged to maximum capacity and depleted to its bare minimum. Thus, the best solution achieved by the suggested technique satisfies all stated goals.
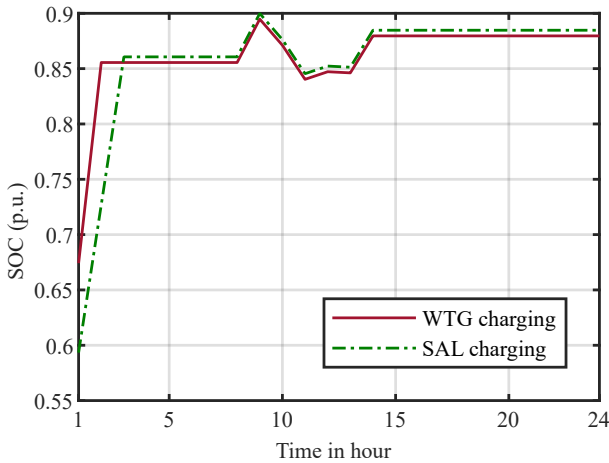
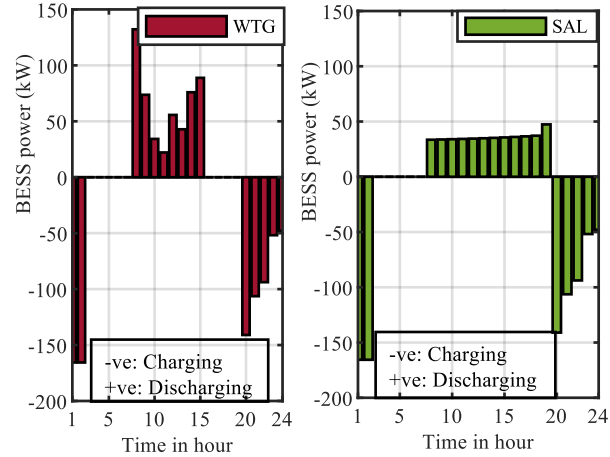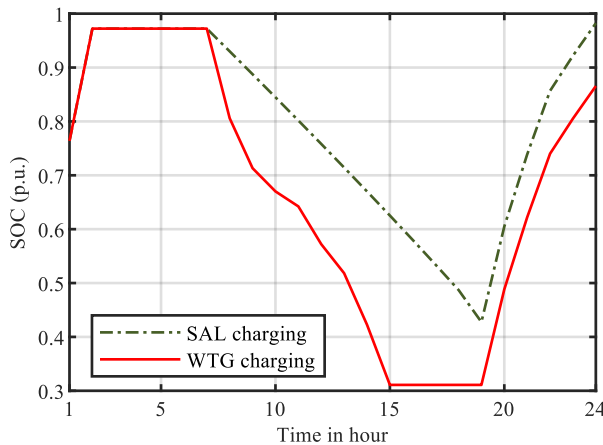**Fig. 20:** SOC of a dispatch cycle of BESS (IEEE-37 bus).

Fig. 21: SOC of a dispatch cycle of BESS (IEEE-25 bus).
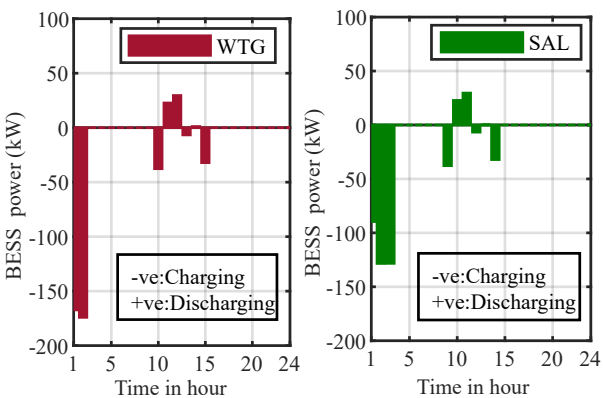
Fig. 22: Status of BESS charging and discharging in a dispatch cycle (IEEE-37 bus).

Fig. 23: Status of BESS charging and discharging in a dispatch cycle (IEEE-25 bus).

RFO algorithm. The proposed framework ensures that the WTG penetrates the distribution system without energy spillage and that the obtained BESS units are utilised optimally. Sustaining average load charging is superior to wind turbine generator charging when the battery storage is free running and draining. It significantly reduces power loss and enhances the system's bus voltage profile by coordinating BESS dispatches with dynamically variable power production from the wind turbine generators and load demand. As a result, the wind turbine generator's successful integration of a BESS system into an unbalanced radial distribution network has been demonstrated. Additionally, this study details the method used to maximise the efficiency of energy storage systems.

Author Contributions

S.P. developed the theoretical formulation, performed the analytic calculations and performed the numerical simulations. M.N. and M.V. supervised the project.

7. Conclusions

The purpose of this work was to propose a novel optimisation framework for determining the optimal placement of wind turbine generators with the BESS system in an unbalanced distribution system using the

References

[1] ADETOKUN, B. B., C. M. MURIITHI and J. O. OJO. Voltage stability assessment and enhancement of power grid with increasing wind energy penetration. *International Journal of Electrical Power & Energy Systems.* 2020, vol. 120, iss. 1, pp. 1–11. ISSN 1879-3517. DOI: 10.1016/j.ijepes.2020.105988.

[2] ALBAKER, A., A. MAJZOOBI, G. ZHAO, J. ZHANG and A. KHODAEI. Privacy-preserving optimal scheduling of integrated microgrids. *Electric Power Systems Research.*

2018, vol. 163, iss. 1, pp. 164–173. ISSN 1873-2046. DOI: 10.1016/j.epsr.2018.06.007.

[3] KIM, J.-C., S.-M. CHO and H.-S. SHIN. Advanced Power Distribution System Configuration for Smart Grid. *IEEE Transactions on Smart Grid.* 2013, vol. 4, iss. 1, pp. 353–358. ISSN 1949-3061. DOI: 10.1109/TSG.2012.2233771.

[4] NADERI, Y., S. H. HOSSEINI, S. G. ZADEH, B. MOHAMMADI-IVATLOO, J. C. VASQUEZ and J. M. GUERRERO. An overview of power quality enhancement techniques applied to distributed generation in electrical distribution networks. *Renewable and Sustainable Energy Reviews.* 2018, vol. 93, iss. 1, pp. 201–214. ISSN 1364-0321. DOI: 10.1016/j.rser.2018.05.013.

[5] SANKUR, M. D., R. DOBBE, A. VON MEIER and D. B. ARNOLD. Model-Free Optimal Voltage Phasor Regulation in Unbalanced Distribution Systems. *IEEE Transactions on Smart Grid .* 2019, vol. 11, iss. 1, pp. 884–894. ISSN 1949-3061. DOI: 10.1109/TSG.2019.2950875.

[6] PINAZO, M. A. and J. L. R. MARTINEZ. Intermittent power control in wind turbines integrated into a hybrid energy storage system based on a new state-of-charge management algorithm. *Journal of Energy Storage.* 2022, vol. 54, iss. 1, pp. 1–21. ISSN 2352-1538. DOI: 10.1016/j.est.2022.105223.

[7] HASSANZADEH, M. E., M. NAYERIPOUR, S. HASANVAND and E. WAFFENSCHMIDT. Decentralized control strategy to improve dynamic performance of micro-grid and reduce regional interactions using BESS in the presence of renewable energy resources. *Journal of Energy Storage.* 2020, vol. 31, iss. 1, pp. 1–16. ISSN 2352-1538. DOI: 10.1016/j.est.2020.101520.

[8] RANA, M. M., M. UDDIN, M. M. R. SARKAR, G. M. SHAFIULLAH, H. MO and M. ATEF. A review on hybrid photovoltaic–Battery energy storage system: Current status, challenges, and future directions. *Journal of Energy Storage.* 2022, vol. 51, iss. 1, pp. 1–20. ISSN 2352-1538. DOI: 10.1016/j.est.2022.104597.

[9] KANG, H., S. JUNG, M. LEE and T. HONG. How to better share energy towards a carbon-neutral city? A review on application strategies of battery energy storage system in city. *Renewable and Sustainable Energy Reviews.* 2022, vol. 157, iss. 1, pp. 1–21. ISSN 1879-0690. DOI: 10.1016/j.rser.2022.112113.

[10] ABDELAZIZ, A. Y., Y. G. HEGAZY, W. EL-KHATTAM and M. M. OTHMAN. Optimal allocation of stochastically dependent renewable energy based distributed generators in unbalanced distribution networks. *Electric Power Systems Research.* 2015, vol. 119, iss. 1, pp. 34–44. ISSN 1873-2046. DOI: 10.1016/j.epsr.2014.09.005.

[11] ASKARZADEH, A. Distribution generation by photovoltaic and diesel generator systems: Energy management and size optimization by a new approach for a stand-alone application. *Energy.* 2017, vol. 122, iss. 1, pp. 542–551. ISSN 1873-6785. DOI: 10.1016/j.energy.2017.01.105.

[12] HASSANZADEHFARD, H, and A. JALIL-IAN. Optimal sizing and location of renewable energy based DG units in distribution systems considering load growth. *International Journal of Electrical Power & Energy Systems.* 2018, vol. 122, iss. 1, pp. 356–370. ISSN 1879-3517. DOI: 10.1016/j.ijepes.2018.03.038.

[13] XING, X, L. XIE and H. MENG. Cooperative energy management optimization based on distributed MPC in grid-connected microgrids community. *International Journal of Electrical Power & Energy Systems.* 2019, vol. 122, iss. 1, pp. 186–199. ISSN 1879-3517. DOI: 10.1016/j.ijepes.2018.11.027.

[14] MOHAMED, A and O. MOHAMMED. Real-time energy management scheme for hybrid renewable energy systems in smart grid applications. *Electric Power Systems Research.* 2013, vol. 122, iss. 1, pp. 133–143. ISSN 1873-2046. DOI: 10.1016/j.epsr.2012.10.015.

[15] BADRAN, O., S. MEKHILEF, H. MOKHLIS and W. DAHALAN. Optimal reconfiguration of distribution system connected with distributed generations: A review of different methodologies. *Renewable and Sustainable Energy Reviews.* 2017, vol. 122, iss. 1, pp. 854–867. ISSN 1879-0690. DOI: 10.1016/j.rser.2017.02.010.

[16] MONTOYA, O. D., J. S. GIRALDO, L. F. GRISALES-NORENA, H. R. CHAMORRO and L. ALVARADO-BARRIOS. Accurate and Efficient Derivative-Free Three-Phase Power Flow Method for Unbalanced Distribution Networks. *Computation.* 2021, vol. 9, iss. 6, pp. 1–21. ISSN 2079-3197. DOI: 10.3390/computation9060061.

[17] SUN, Y., T. DING, T. XU, C. MU, P. SIANO and J. P. CATALAO. Power Flow Analytical Method for Three-Phase Active Distribution Networks Based on Multi-Dimensional Holomorphic Embedding Method. *IEEE Transactions on Circuits and Systems II: Express Briefs.* 2022,

vol. 69, iss. 12, pp. 5069–5073. ISSN 1558-3791. DOI: 10.1109/TCSII.2022.3204606.

[18] WANG, C., Z. ZHANG, O. ABEDINIA and S. G. FARKOUSH. Modeling and analysis of a microgrid considering the uncertainty in renewable energy resources, energy storage systems and demand management in electrical retail market. *Journal of Energy Storage.* 2021, vol. 33, iss. 1, pp. 1–13. ISSN 2352-1538. DOI: 10.1016/j.est.2020.102111.

[19] RAMADAN, A., M. EBEED, S. KAMEL, E. M. AHMED and M. TOSTADO-VELIZ. Optimal allocation of renewable DGs using artificial hummingbird algorithm under uncertainty conditions. *Ain Shams Engineering Journal.* 2022, vol. 14, iss. 2, pp. 1–14. ISSN 2090-4495. DOI: 10.1016/j.asej.2022.101872.

[20] SHOJAEI, S., J. BEIZA, T. ABEDINZADEH and H. ALIPOUR. Optimal energy and reserve management of a smart microgrid incorporating parking lot of electric vehicles/renewable sources/responsive-loads considering uncertain parameters. *Journal of Energy Storage.* 2022, vol. 55, iss. 2, pp. 1–14. ISSN 2352-1538. DOI: 10.1016/j.est.2022.105540.

[21] OLADEJI, I., R. ZAMORA and T. T. LIE. Optimal allocation of energy storage system and its benefit analysis for unbalanced distribution network with wind generation. *Sustainable Energy, Grids and Networks.* 2022, vol. 32, iss. 1, pp. 1–14, ISSN 2352-4677. DOI: 10.1016/j.segan.2022.100897.

[22] PATNAIK, S, S. RAY, K. KASTURI and M. R. NAYAK. Optimal allocation of DGs for non-linear objective function modeling in a three-phase unbalanced distribution system using crow search optimization algorithm. *Journal of Interdisciplinary Mathematics.* 2022, vol. 25, iss. 3, pp. 681–701. ISSN 0972-0502. DOI: 10.1080/09720502.2021.2012894.

[23] SHAABAN, M. F., M. H. AHMED, M. M. A. SALAMA and A. RAHIMI-KIAN. Optimization unit for real-time applications in unbalanced smart distribution networks. *Journal of advanced research.* 2019, vol. 20, iss. 1, pp. 51–60. ISSN 2090-1224. DOI: 10.1016/j.jare.2019.04.001.

[24] TENG, J.-H. and C.-Y. CHANG. A novel and fast three-phase load flow for unbalanced radial distribution systems. *IEEE Transactions on Power Systems.* 2002, vol. 17, iss. 4, pp. 1238–1244. ISSN 1558-0679. DOI: 10.1109/TPWRS.2002.805012.

[25] POLAP, D. and M. WOZNIAK. Red fox optimization algorithm. *Expert Systems with Applications.* 2021, vol. 166, iss. 1, pp. 1–21. ISSN 1873-6793. DOI: 10.1016/j.eswa.2020.114107.

About Authors

Samarjit PATNAIK was born in Bhubaneswar, India. He received his M.Tech. from Indian Institute of Technology Kharagpur in 2012. His research interests include Grid integration of renewable energy sources and power system planning.

Manas Ranjan NAYAK received Ph.D. degree from Electrical Engineering Department of Siksha 'O' Anusandhan University, Bhubaneswar. He is currently a professor at CAPGS, Biju Patnaik University of Technology, Rourkela, Odisha. His research interest includes Renewable Energy, Energy Storage System, Electric Vehicle, and its integration in distribution system, Power system planning, Optimization techniques.

Meera VISWAVANDYA received Ph.D. degree from Electrical Engineering Department of Utkal University, Bhubaneswar. She is currently a professor at Odisha University of Technology and Research, Bhubaneswar, Odisha. Her research interests are Renewable Energy, control Systems and its integration in distribution system.

Appendix A   BESS Parameters

- Battery type = Lithium-ion deep cycle,
- Battery make = KW-LCP-48.500,
- Power output = 20 kW,
- Energy capacity = 24 kWh,
- Round trip efficiency = 80 %,
- Self-discharge factor = $1 \cdot 10^{-5}$,
- Charging temperature = $0°$C to $45°$C,
- Discharging temperature = $-20°$C to $60°$C,
- Battery life span = 10 yrs,
- $SOC^{\max}$ = 90 %,
- $SOC^{\min}$ = 20 %,
- Initial SOC = 50 %.